Foredune blowout formation and subsequent evolution along a chronically eroding high-energy coast

Quentin Laporte-Fauret, Bruno Castelle, Vincent Marieu, Alexandre Nicolae-Lerma, David Rosebery

Title: Foredune blowout formation and subsequent evolution along a chronically eroding high-energy coast.

Quentin Laporte-Fauret[1]*, Bruno Castelle[1], Vincent Marieu[1], Alexandre Nicolae Lerma[2,3], David Rosebery[4]

[1] Univ. Bordeaux, CNRS, Bordeaux INP, EPOC, UMR 5805, F-33600 Pessac, France
[2] BRGM, Regional Direction Nouvelle Aquitaine, 24 avenue Leonard de Vinci, 33600, Pessac, France
[3] OCNA, Observatoire de la Côte de Nouvelle Aquitaine
[4] Office National des Forêts, 75570 CEDEX 12 Paris, France

* Corresponding author. Tel.: +33-540-003-316
email: quentin.laporte-fauret@u-bordeaux.fr;

Highlights

- Orthophoto, Lidar and UAV surveys allow to assess multi-decade coastal dune changes
- Blowouts preferably develop where marine erosion is the most intense
- Blowouts promote the transport of windblown sand to the back of the dune
- Erosion scarp, paleosols and vegetation prevent landward transport
- Blowouts can help maintaining dune systems in chronically eroding dune systems

Abstract

Coastal dune systems provide important ecosystem services, while being vulnerable to marine erosion. In these environments, blowouts can develop and promote sand transport from the beach to the back of the dune, but are generally fought by coastal dune managers. There are only few quantitative studies on the 3D evolution of blowouts and how they can develop into parabolic dune. We investigate the morphological evolution of a 2-km long freely evolving dune system in southwest France from 1947 to 2021 using historical aerial photos and digital surface models from Lidar and UAV photogrammetry. The combination of these remote sensing methods shows an alongshore non-uniform erosion with a mean of 1.26 m/yr, and with erosion rates in the north of the study area four times larger than in the south. Over the study period, three large blowouts developed in the northern, (more rapidly eroding) sector and subsequently evolved into parabolic dunes, with a depositional lobe migrating landward into the forest. Two parabolic dunes naturally stabilized by vegetation colonization, without any reactivation phase, with the third one still migrating landward with an average migration of 7.2 m/yr. A high-frequency and high-resolution analysis of the active blowout was performed between 2014 and 2021. Compared to the adjacent areas, this blowout promoted dune landward migration. Since 2014, the high erosion scarp in the adjacent southern sector prevented the transport of sand resulting in a loss of dune volume due to marine erosion. In contrast, in the adjacent northern sector and in front of the blowout, the presence of vegetation and paleosols at the dune toe favored sand deposition and limited marine erosion. In chronically eroding sectors, promoting blowouts and thus landward dune migration may be considered as an efficient management approach to maintain the dune system.

Keywords: Coastal dune; Remote sensing; Marine erosion; Blowout; Parabolic dune.

1. Introduction

With increased anthropic pressure (e.g., demographic expansion of coastal areas, Neumann et al., 2015; Merkens et al., 2018) and climate change (e.g., sea level rise and increase in storminess, Zappa et al., 2013; Cazenave et al., 2014), sandy coasts (31% of the world coastlines, Luijendijk et al., 2018) are among the most vulnerable environments. In the backshore and landwards of sandy beaches with sufficient sand supply, coastal dunes can develop through many interactions between marine and aeolian processes on the one hand (Nordstrom, 2000; Hesp, 2002; Cohn et al., 2018), and vegetation growth and burial on the other hand (Maun, 1998; Maun and Perumal, 1999; Zarnetske et al., 2012). Dune vegetation traps windblown sand and promotes sand deposition, which, in turn, can promote plant growth. This positive feedback is responsible for the growth of coastal dunes along many coasts worldwide (Maun, 1998; Emery and Rudgers, 2014; Charbonneau et al., 2021). As coastal dunes develop, they provide new habitats that promote plant succession, eventually stabilizing the dune system (Barbour et al., 1985; Provoost et al., 2011; Pye et al., 2014; Charbonneau et al., 2016). Coastal dunes also provide ecosystem services such as natural and effective barrier against flooding and storm waves, the formation of ecological niches for plants, the filtration of pollutants, fresh water supply or the expansion of nesting sites (Martinez et al., 2013).

Foredune blowouts are erosional features typical of active dune systems (Black, 1951; Adamson et al., 1988). These depressions, formed by wind erosion, are characterized by a deflation basin, erosion walls, and a deposition lobe (Glenn, 1979; Carter et al., 1990; Hesp, 2002). Foredune blowouts can be classified into two broad categories according to their morphologies: saucer blowouts and trough blowouts (Cooper, 1958; Cooper, 1967). The formers are shallow with a circular shape while the latter are more elongated, deeper and with a well-defined deposition lobe. Blowouts are an important component of dune functioning. Under strong onshore wind, the airflow is topographically accelerated through the deflation basin, it erodes the base of the deflation basin and transports the sand into the deposition lobe or beyond to the back dune (Hesp and Hyde, 1996; Fraser et al., 1998; Pease and Gares, 2013). These new deposits generate a disturbance for plants species that can lead to a local vegetation rejuvenation (Nordstorm et al., 2007, Laporte-Fauret et al., 2021a; Laporte-Fauret et al., 2021b) and a vertical accretion potentially increasing the back dune resilience to sea-level rise and coastal erosion (Clemmensen et al., 2001; Hesp, 2002; Petersen et al., 2005; Rhind and Jones, 2009; Arens et al., 2013; Hesp and Hilton, 2013; Martinez et al., 2013; Kuipers, 2014; Jewell et al., 2017; Pye and Blott, 2017). For this reason, in recent years (natural or artificial) blowouts have been progressively considered as a potential means for efficient management approach in some regions of the world (Van Boxel et al., 1997; Arens et al., 2013; Kuipers, 2014; Pye and Blott, 2016; Ruessink et al., 2018; Laporte-Fauret et al., 2021b). In particular, naturally (or artificially) stabilized dune systems threatened by chronic marine erosion can be remobilized and migrate landward through blowout development which, in sector under severe shoreline erosion, may maintain the dune system (Castelle et al., 2019).

Many studies on blowouts have focused on the airflow modification, including acceleration and steering, using two- and three-dimensional anemometers (Hesp and Hyde, 1996; Hugenholtz and Wolfe, 2009; Hesp and Walker, 2012; Pease and Gares, 2013) and computational fluid dynamics (Jackson et al., 2011; Smyth et al., 2012) by predominantly focusing on the short-term (event) scale. Studies on morphological changes on medium (months) to long (annual/decadal) temporal scales, are scarcer and focus mainly on planview (horizontal) changes using erosion pins, aerial photography or ground penetrating radar (Jungerius and van der Meulen, 1989; Gares and Nordstrom, 1995; Hugenholtz and Wolfe, 2006; González-Villanueva et al., 2011; Abhar et al., 2015; Jewell et al., 2017).

Blowout evolution depends on complex interactions between abiotic (e.g., windblown sand, marine erosion) and biotic (e.g., vegetation colonization and growth) processes (Gares and Nordstrom, 1995; Hesp, 2002; Pye and Blott, 2017). Schwarz et al. (2018) developed a conceptual model of blowout evolution highlighting these bio-geomorphological interactions according to three stages. Blowout initiation (Stage 1) is dominated by abiotic (aeolian) processes that increase the size and depth of the blowout. Blowout development (Stage 2) is governed by bio-geomorphological interactions between vegetation development, which inhibits blowout extension, and physical disturbance, which inhibits vegetation development. Finally, closure (Stage 3) is related to biotic processes where vegetation development prevents erosion and promotes deposition in the blowout. However, in stormy environments the constant erosion of the erosion walls, by avalanches of sediment from the crest to the deflation basin, generates significant sedimentary supplies that further feed the deposition lobe. If the disturbance remains too large for vegetation colonization, the lobe may continue to migrate downwind leading to the development of hairpin or long-walled parabolic dunes with trailing arms (Melton, 1940; Cooper, 1958; Wiedemann, 1991; Hesp, 2001; Girardi and Davis, 2010). The size of the parabolic dune may continue to increase if enough sand supply through the deflation basin is sustained. In contrast, the growth may cease if the deflation basin becomes too large, preventing airflow acceleration and sand transport; if it reaches a non-erodible layer (e.g., ground water table, limestone bed, or paleosol); or if it becomes colonized by vegetation (Melton, 1940; Cooper, 1958; Livingstone and Warren, 1996, Hesp, 2002). Yan and Baas (2015) highlighted approximatively 20 studies documenting the formation of parabolic dunes from blowout. Most of these studies were based on field surveys, aerial photo interpretation on multi-year to decadal time scales (see Table 4 in Yan and Baas, 2015), or numerical modeling (Baas and Nield, 2007; Nield and Baas, 2008). However, as shown by Delgado-Fernandez et al. (2018), large morphological evolutions can take place on very short time scales (e.g., storm event). Therefore, there is a real lack of quantitative studies at high spatial resolution and on time scales ranging from event to decade on blowouts transformation into parabolic dune.

The objective of this study is to investigate the morphological evolution of a freely evolving dune system dissected by many natural blowouts in a chronically eroding sector in southwest France. These investigations are carried out using historical aerial photos to understand these evolutions since 1947 and Digital Surface Models (DSMs) performed by Lidar and UAV photogrammetry on event to seasonal timescales in order to provide fresh and quantitative insight into the 3D dune evolution, focusing on an active blowout that recently developed into a parabolic dune.

2. Material and methods

2.1. Study site

The study site, l'Anse du Gurp, is located in the northern part of an almost uninterrupted 110-km dune system along the Gironde coast, southwest of France (Figure 1.a). This coast is mainly characterized by open sandy beaches facing W-WNW, turning to WNW-facing to the north at the Pointe de la Négade. The coast is meso- to macro-tidal with an average tidal range of 3.7 m, reaching a maximum of 5 m during spring tides (Castelle et al., 2015, measured at the Arcachon-Eyrac tide gauge, Figure 1.a). The beaches are exposed to an energetic wave climate with waves generated in the North Atlantic Ocean arriving with a dominant W to NW incidence. Incident waves show strong seasonal variability with monthly averages of significant wave heights (*Hs*) and period between peaks (*Tp*) ranging from 1.1 m and 8.5 s in July with a dominant W-NW direction, to 2.4 m and 13 s in January with a dominant W direction (Castelle et al., 2017, measured at the wave buoy, Figure 1.a). This strong seasonal variability is also found in the wind conditions with an average hourly mean wind speed and direction of 4.5 m/s and 311° (NW) in summer and 5.2 m/s 263° (W) in winter, potentially exceeding 36 m/s during extreme storms (Laporte-Fauret et al., 2021b, measured at the weather station, Figure

1.a). Winter (wind and waves) conditions also show a large interannual variability due to large-scale climate patterns of atmospheric variability. The West Europe Pressure Anomaly (WEPA) was found to be a dominant mode explaining the winter interannual variability in the Bay of Biscay of e.g., westerly winds, wave height, precipitations, river discharge (Castelle et al., 2017; Jalón-Rojas and Castelle, 2021). The positive phase of WEPA reflects a southward-shifted and intensified Icelandic Low / Azores funneling high-energy waves and storm winds towards the Bay of Biscay (Castelle et al., 2017).

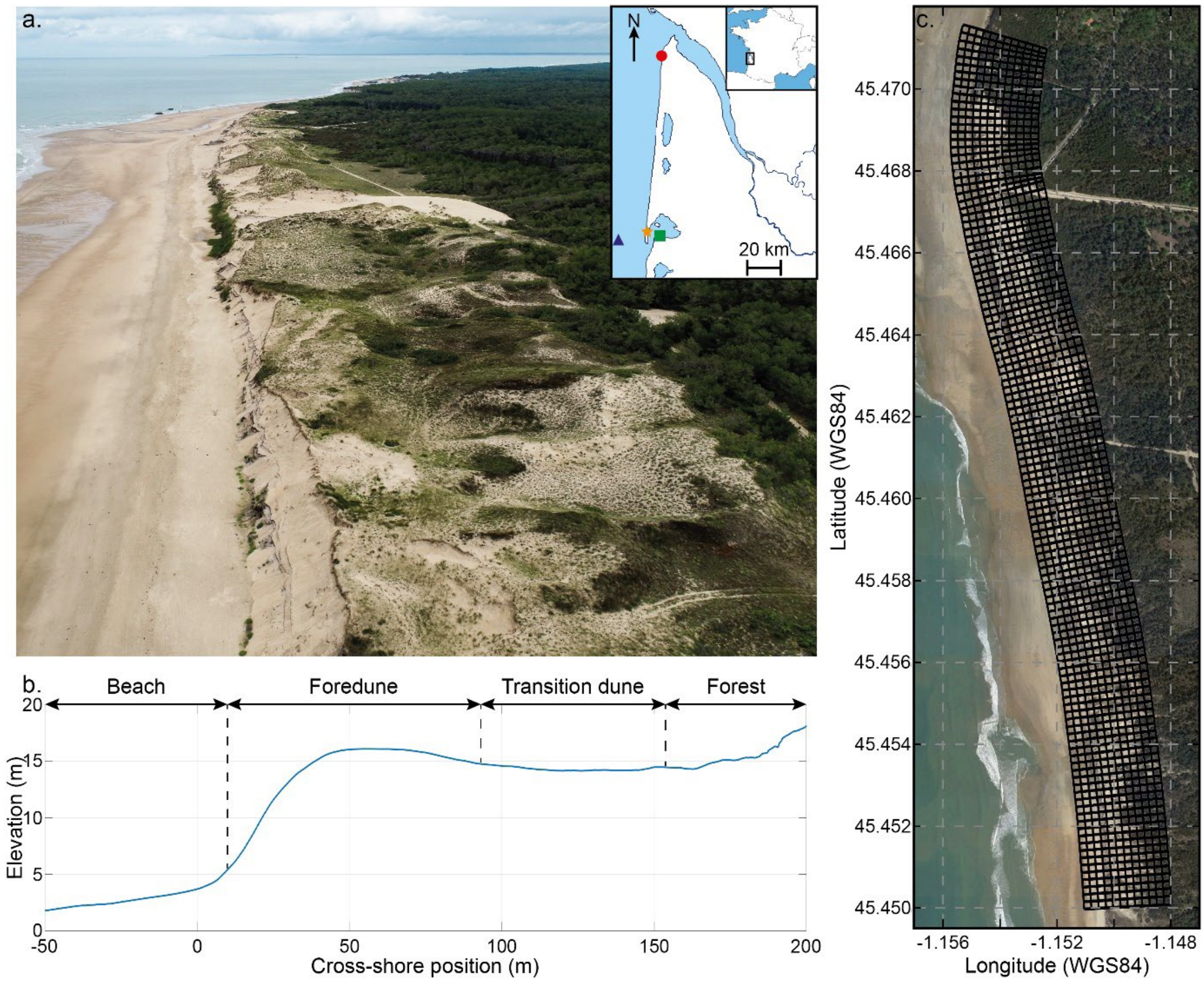

Figure 1. (**a**) Aerial photograph of l'Anse du Gurp (Ph. Quentin Laporte-Fauret), the red bubble, the green square, the blue triangle and the orange star show the location of the study site, the Arcachon-Eyrac tide gauge, the wave buoy and the weather station, respectively, (**b**) 2 km alongshore-averaged beach dune profile at l'Anse du Gurp, (**c**) 2 km curvilinear grid used at l'Anse du Gurp.

At l'Anse du Gurp, the dune system, located between the beach and the forest, is composed of a foredune and a transition dune, both showing large alongshore variability, reaching a mean height of 16 m with a mean width of 85 m (Figure 1.b). The dune system is composed of medium grain sand from 300 µm to 415 µm (Bosq et al., 2019; Stéphan et al., 2019). The overall shape of the dune is largely inherited from the action of the coastal stakeholders who built the dune systems using fences and vegetation planting from the 19th century (Buffault, 1942, Bossard and Lerma, 2020; Robin et al., 2020). Unlike some other dune systems where soft engineering methods are still applied (e.g., Truc Vert, Laporte-Fauret et al., 2021b), the dune system at l'Anse du Gurp has not been managed since the early 2000s. This area is characterized by a chronic, quasi-steady, erosion since the 1950s (Castelle et al., 2018), which prevents the formation of incipient foredune and generates high erosion cliffs. It is a remote system, with only an old and partially destroyed concrete road dating from the German occupation. However, despite access is prohibited, the area is often used as attested by paths formed by animals, hunters, dissident walkers and even motocross riders (see Figure 4.i). Finally, the dune system is perched on Pleistocene paleosols, which are more resistant to marine erosion than sand and locally outcrop at the dune toe and/or upper part of the beach, particularly after high-energy winters (Pontee et al., 1998; Castelle et al., 2015; Stéphan et al., 2019).

2.2. Data

A set of 6 B&W and 3 RGB historical aerial photographs covering the study area were collected from the French National Institute of Geography and Forest Information (IGN) (Table 1). These surveys cover the period from 1947 to 2012, with a quasi-decadal frequency during the 1900s and then approximately every four years in the 2000s, with a pixel size ranging from 0.33 m to 1.87 m.

Table 1. Characteristics of the aerial photo survey dataset from 1947 to 2012.

Date	Number of photos	Color data	Pixel size (m)
1947-05-29	6	B&W	1.12
1957-06-18	9	B&W	1.87
1969-01-01	9	B&W	0.84
1977-09-10	7	B&W	0.87
1986-07-18	6	B&W	1.33
1998-06-24	22	B&W	0.33
2004-06-14	5	RGB	1.62
2009-06-23	8	RGB	0.79
2012-08-08	14	RGB	0.46

For each survey, all the photos were assembled and merged using Agisoft Metashape (v1.7.2) in order to build a 3D georeferenced model and an orthomosaic following a 4-step workflow, (1) the cameras were aligned by the detection of matching points on overlapping image parts, (2) the 3D sparse point cloud, generated by the camera alignment, was orthorectified using 13 fixed Ground Control Points (GCPs, e.g., crossroads) from the recent IGN referenced images and a camera optimization procedure was performed to compute the intrinsic camera calibration parameters by minimizing the error on the ground control points, (3) a 3D dense point cloud was generated and (4) interpolated with Matlab on a 0.2 x 0.2 m regular grid (Figure 1.c) in order to build a textured DSM that can be exploited in geographic, projected, or local (cross-shore/longshore) coordinates. The planimetric errors of DSMs from historical aerial photos are under 3 m.

Two topographic surveys performed by airborne Lidar on the entire Aquitaine coast were used, the first dated October 23-24, 2014 with a density of 4 points/m² and an altimetric error of 0.14 m (Lerma et al., 2019), and the second dated October 07, 2021, with a density of 15 points/m² and an altimetric error of 0.10 m. The second Lidar survey was mainly used to estimate the DSM error due to vegetation coverage, in particular at the parabolic dune toe. From January 2016 to January 2018, 17 surveys were performed using a DJI Phantom 2 (DP2) quadricopter UAV equipped with 12MPix camera (GoPro Hero 4 Black), and, from November 2018 to July 2021, four surveys were performed using a DJI Phantom 4 Pro (DP4P) quadricopter equipped with a 20MPix camera. All surveys were performed according to the monitoring strategy designed and validated in Laporte-Fauret et al. (2019). In short, the surveys covered 2 km of beach/dune system with an automatized fly plan. In order to georectify the DSM, an array of 14 permanents GCPs were implemented by pairs (one in the foredune and one in the transition dune) every

250 m alongshore. Their positions were measured with GNSS before each winter. The DSM generation process follows the same workflow as the one applied to the historical aerial photos except that the rectification is done with the permanent GCPs instead of crossroads. Laporte-Fauret et al. (2019) showed that this protocol leads to altimetric RMSE around 0.13 m and 0.05 m for DP2 and DP4P, respectively. Given the curvature of the coast, here the DSMs were computed on a curvilinear, cross-shore/longshore, grid (Figure 1.c).

2.3. Coastal dune metrics

There is a large range of shoreline definitions (Boak and Turner, 2005). In our study, in line with previous work in southwest France (Castelle et al., 2017; Lerma et al., 2019), from the LiDAR and UAV DSMs we computed the shoreline position the iso-contour $z = 5.5$ m, which correspond to the dune toe on almost the entire site. Given the poor altimetric accuracy of the historical DSMs, the shoreline position was digitized by an operator. Given the curvilinear grid used for DSM generation, the dune volume from 2014 to 2021 was computed as:

$$V = \sum_{j=j_S}^{j_N} \sum_{i=i_W}^{i_E} S_{ij}(z_{ij} - z_{DT}) \tag{1}$$

where j_S and j_N are the grid indices of the southern and northern limit, respectively, i_W and i_E are the grid indices of the western and the eastern limit, respectively. i_W is defined as the shoreline position index of the dune toe and i_E is defined as the forest limit index, manually digitized on the last drone survey (2021-07-09). S_{ij} and z_{ij} are the grid cell surface and elevation at grid point (i,j), respectively and z_{DT} is the elevation of the dune toe. The evolution of the alongshore-averaged dune volume through the survey was computed as:

$$DV = \frac{V_i - V_0}{d_{SN}} \tag{2}$$

where DV is the dune volume difference per beach width (m^3/m) between the dune volume of the date i (i.e., V_i) and the initial dune volume (i.e., V_0) computed from the Lidar 2014, and d_{SN} is the alongshore distance between the northern (i.e., j_N) and the southern (i.e., j_S) limits. All calculations were performed using the curvilinear grid shown in Figure 1.c, which allows straightforward computations of alongshore-averaged quantities. The cross-shore position $x = 0$ m corresponds to the shoreline position measured in the field along the 110-km Gironde coast using a DGPS-equipped ATV on 2014-11-14 (Castelle et al., 2015). The models generated by Lidar data and UAV photogrammetry are Digital Elevation Model (DEM) and DSM, respectively. In order to correct the DSM-DEM bias, the 2017-10-04 airborne Lidar (DEM) survey and the 2017-10-26 UAV photogrammetric (DSM) survey were compared, showing an average 0.1-m vertical difference in the vegetated areas. Hence the 2014 initial volume V_0 was corrected by rising the DEM elevation by 0.1 m in vegetated areas of the dune, in order to be consistent with subsequent photogrammetric DEMs. From the October 26, 2017 survey, a dense vegetation zone started to develop in front of the parabolic dune, which could alter the volume computation with the DSMs. By comparing the UAV-DSM of July 9, 2021 and the Lidar-DEM of October 07, 2021, the vegetation was outlined and its volume computed. Then its effect on the elevation was calculated as:

$$D_z = \frac{V_{UAV} - V_{Lidar}}{S_{veg}} \tag{3}$$

where V_{UAV} and V_{Lidar} are the volume of the outlined vegetation for the UAV-DSM and the Lidar-DEM, respectively and S_{veg} is the surface of the outlined vegetation. Then, for each DEM from October 26, 2017, the vegetation was outlined and then a correction was applied by:

$$V_{corrected} = V - (S_{veg}\, D_z) \tag{4}$$

where V and S_{veg} are the initial volume and the vegetation surface for each survey, respectively.

3. Results

3.1. Long term spatial coastal dune evolution

Figure 2.a shows the time series of shoreline position from 1947 to 2021, highlighting chronic, quasi-steady, marine erosion. The shoreline erosion rate increases northwards, from 0.68 m/yr in the south to 2.72 m/yr in the north (Figure 2.b). Erosion rates are fairly uniform alongshore in the south of the study zone, before dramatically increasing northwards in the northern part (Figures 2 and 3).

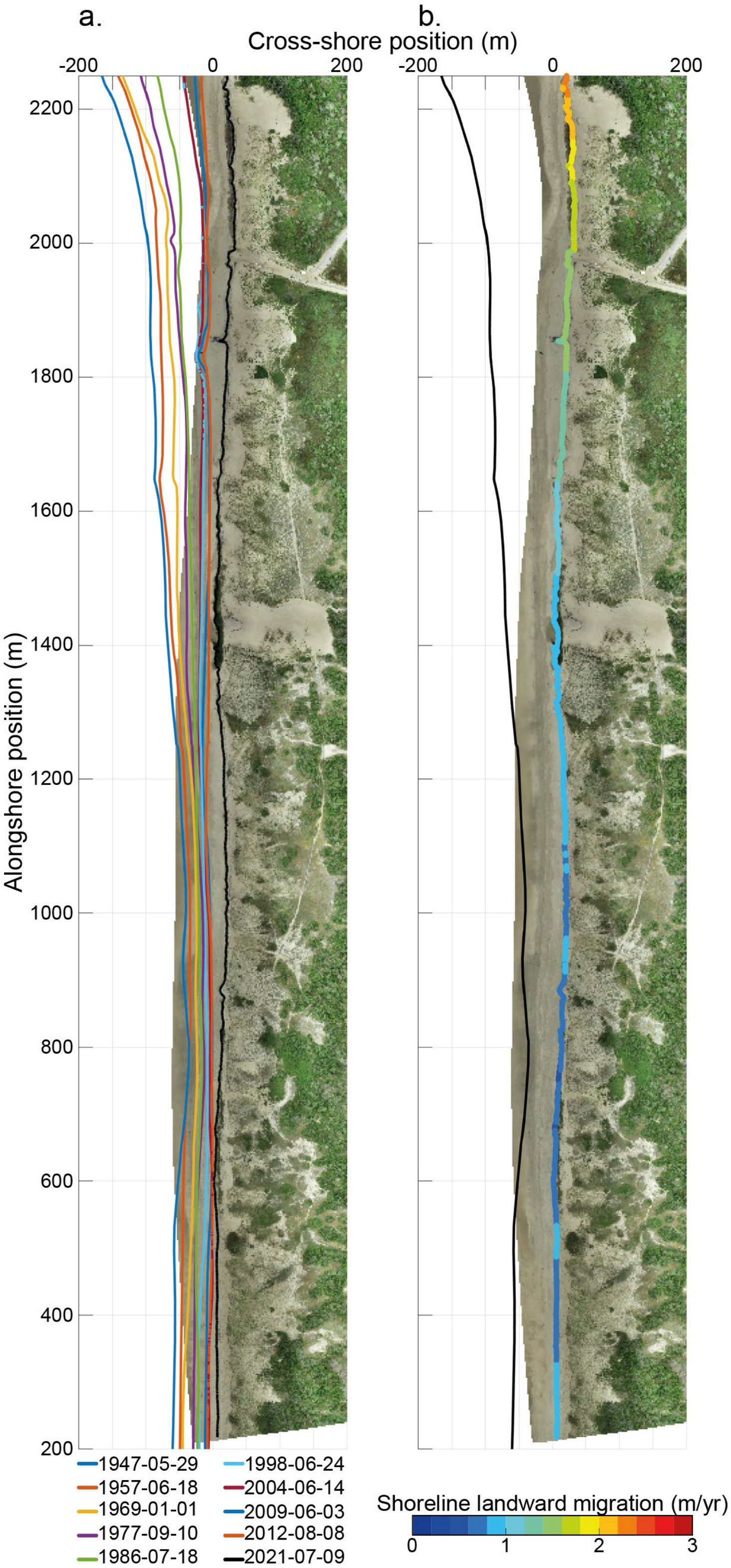

259
260 Figure 2. Orthophotos of l'Anse du Gurp in 2021-07-09 with superimposed (**a**) shorelines from 1947-
261 05-29 to 2021-07-09 and (**b**) colored shoreline migration rate computed from 1947-05-29 (black line)
262 to 2021-07-09 (colored line).
263

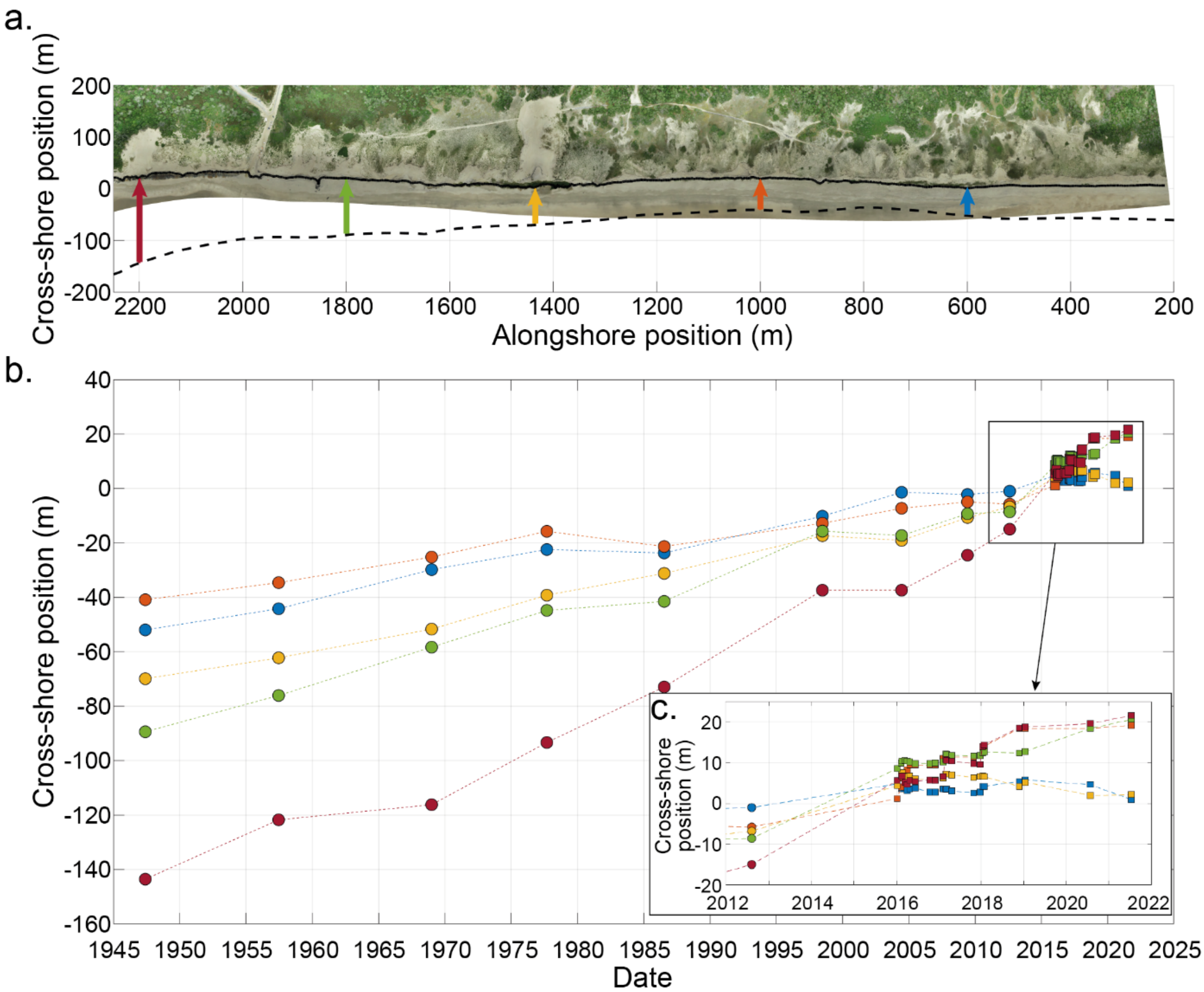

Figure 3. (**a**) Orthophotos of l'Anse du Gurp on 2021-07-09 with shoreline position (black line) and the shoreline position on 1947-05-29 (black dashed line). The five colored arrows represent the shoreline migration at five alongshore position $x = 600$ m (blue), $x = 1000$ m (orange), $x = 1435$ m (yellow), $x = 1800$ m (green) and $x = 2200$ m (red), (**b**) time series of the shoreline cross-shore position for these 5 alongshore positions from 1947-05-29 to 2021-07-09 with (**c**) a zoom on the 10 last years. Circles and squares represent data from aerial photography and UAV photogrammetry, respectively.

All the orthophotos since 1947 show a coastal dune system systematically dissected by breaches and blowouts (Figure 4), with the notable successive development and evolution of three large blowouts (i.e., $x = 1450$ m, $x = 1850$ m and $x = 2200$ m) at different times from 1977 (white rectangles in Figure 4.d-j). The first breach ($x = 1850$ m) formed around 1977 (Figure 4.d) and further developed into a large blowout around 2004 (Figure 4.g). The deposition lobe migrated landward before reaching the forest in 2009 (Figure 4.h) and further stabilizing and revegetating after 2012 (Figure 4.i,j,k). The second blowout ($x = 2200$ m) rapidly developed between 2004 and 2012 (Figure 4.g,h,i) when its deposition lobe reached the forest. Incipient vegetation colonized the southern part of the blowout starting in 2016 (Figure 4.j) and subsequently extending to 2021 (Figure 4.k) suggesting no further morphological development. Finally, the third blowout ($x = 1450$ m) shows an initial development concurrent to the previous one (Figure 4.g,h), with the formation of a deflation basin between two vegetated erosion walls, and a large deposition lobe. Compared to the two other blowouts, this blowout is located in a sector with less intense chronic erosion and a wider dune system. The deposition lobe continuously grows, with a quasi-steady landward migration into forest between 2016 (Figure 4.j) and

2021 (Figure 4.k). As erosion walls remained vegetated and stable, this blowout transformed into a parabolic dune which will be analyzed in detail in Section 3.2.2.

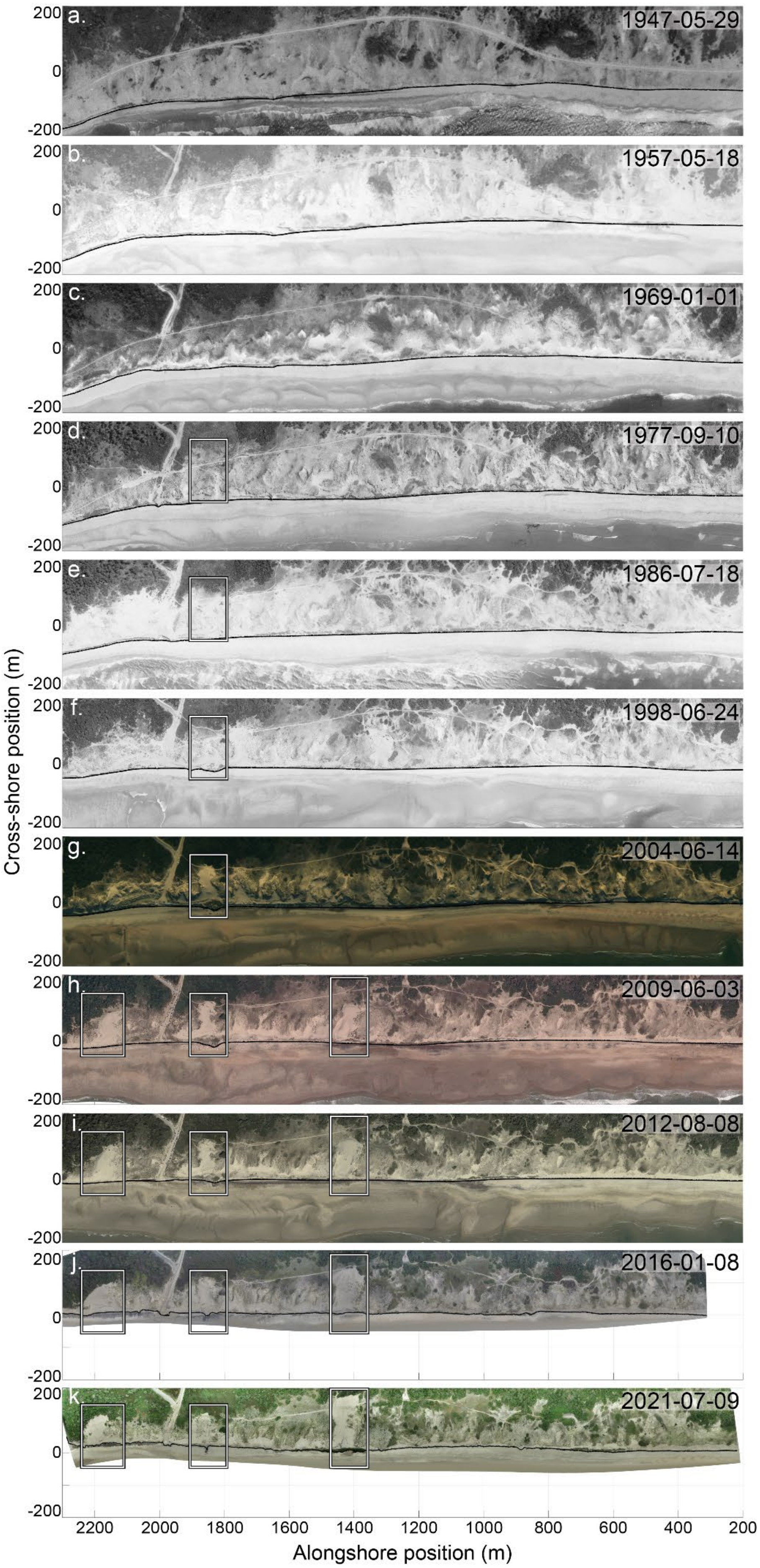
a.
1947-05-29
b.
1957-05-18
c.
1969-01-01
d.
1977-09-10
e.
1986-07-18
f.
1998-06-24
g.
2004-06-14
h.
2009-06-03
i.
2012-08-08
j.
2016-01-08
k.
2021-07-09
200
0
-200
Cross-shore position (m)
2200 2000 1800 1600 1400 1200 1000 800 600 400 200
Alongshore position (m)

290

Figure 4. (**a-i**) Aerial orthophotos of l'Anse du Gurp and (**j-k**) UAV orthophotograph, all represented in the local coordinate system. The black line represents the shoreline position for each date and the white rectangles indicate the position of large blowouts.

3.2. Coastal dune morphological evolution

3.2.1. Overall dune system

The dune system of l'Anse du Gurp is strongly non-uniform alongshore due to the presence of many breaches cutting the dune, with different sizes and shapes, some of them starting to develop into trough or saucer blowouts. Between 2016 (Figure 5.a) and 2021 (Figure 5.b), three large blowouts developed in this 2-km long dune system, at $x = 1435$ m, $x = 1850$ m and $x = 2200$ m. The DSM difference between 2016 and 2021 (Figure 5.c) highlights two large areas of dune marine erosion with an average (maximum) vertical erosion of 6 m (11 m). These areas are located between $x = 850$ m and $x = 1350$ m with horizontal dune toe erosion reaching 20.8 m, and further north, between $x = 1625$ m and $x = 2250$ m, where the average (maximum) vertical erosion is 10 m (15 m) with horizontal dune toe erosion reaching 33.8 m. The blowouts at $x = 1435$ m and $x = 2200$ m show an average vertical erosion of 3 m in the deflation basin, reaching 6 m in the center, whereas the blowout at $x = 1850$ m shows lower vertical erosion with an average of 1.5 m, reaching 3.5 m in the center. Apart from these active blowouts, the foredune is mainly characterized by vertical accretion with an average (maximum) of 0.4 m (1.5 m) between $x = 320$ m and $x = 1350$ m, and 0.8 m (2.1 m) between $x = 1480$ m and $x = 1950$ m. The largest vertical accretion values are found in the deposition lobe of the three main blowouts with an average (maximum) of 2 m (5 m) at $= 1435$ m, 2 m (4 m) at $= 1850$ m and 1 m (3 m) at $= 2200$ m. The dune system of l'Anse du Gurp has been continuously losing sand since 2014 (Figure 6.b) with winter marine erosion exceeding the amount of sand recovered in spring-summer-fall. This results in a net loss of sand of 70.7 m^3/m between 2014 and 2021, i.e., 4.98% of the total volume with a mean rate of 10.5 m^3/m/yr (Figure 6.a,b).

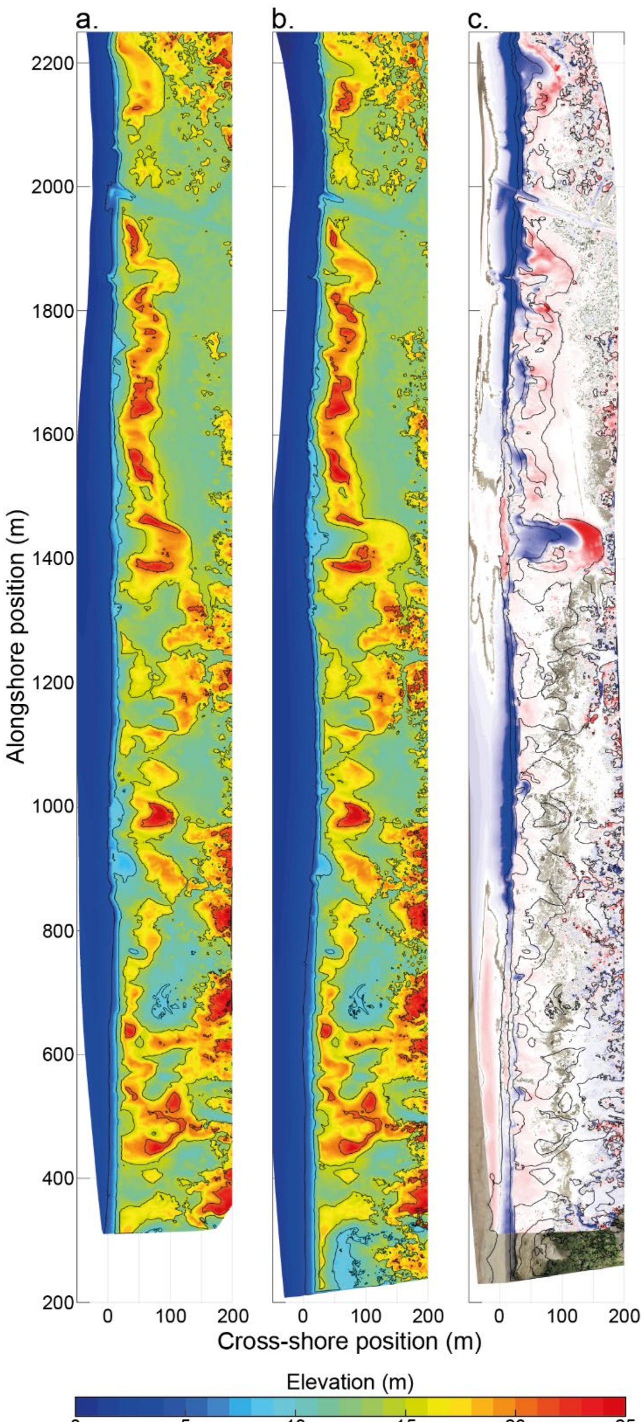

Figure 5. DSM of l'Anse du Gurp in (**a**) 2016-01-08 and (**b**) 2021-07-09 and (**c**) and corresponding difference plot.

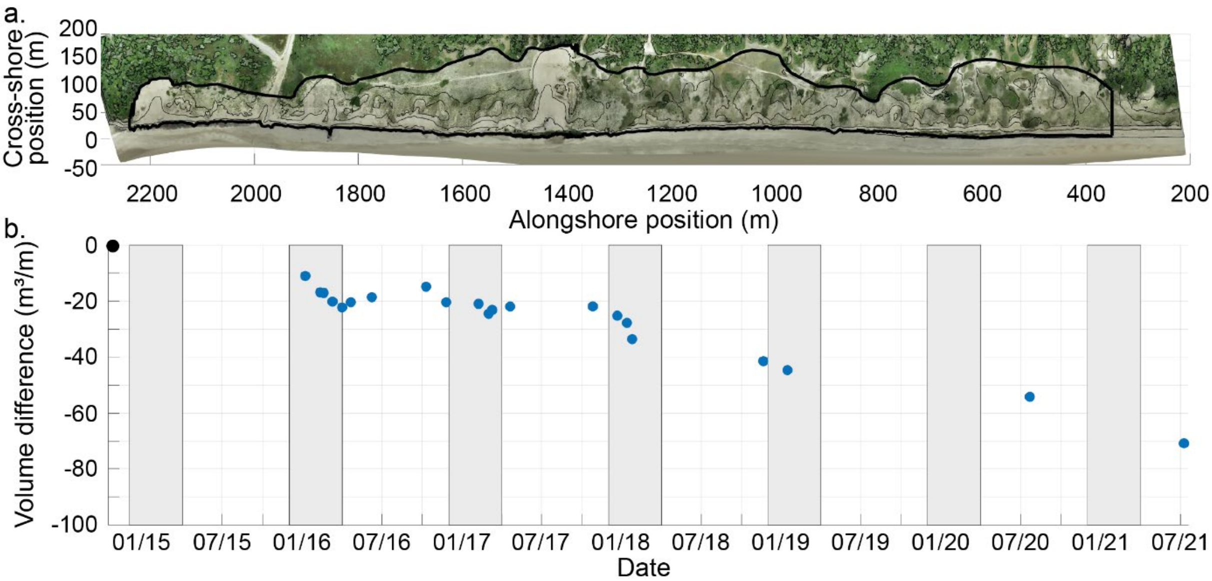

Figure 6. (**a**) UAV-derived orthophotograph of l'Anse du Gurp in 2021-07-09 where the black lines delimit the area in which the volumes are calculated, (**b**) Time series of the volume difference between 2014 and 2021. Grey rectangles represent the winter periods, blue and black points are for drone and Lidar surveys, respectively.

3.2.2. Zoom onto the parabolic dune

As revealed by the historical aerial photos (Figure 4), the blowout that formed after 2004 (Figure 4.g-k) has evolved into a parabolic dune (Figure 7). Figure 8 shows the high-frequency morphological evolution of this blowout from 2016 to 2021. In 2016, the distances between the base of the erosion walls and from the throat to the end of the deposition lobe were 40 m and 118 m, respectively. After 5.5 years of monitoring, the parabolic dune is still mostly unvegetated, which is characteristic of the first stage of the Schwarz et al. (2018) blowout development model, indicating that its current evolution is mainly related to physical forcing. Indeed, the deposition lobe continuously migrated landward with concurrent widening of the deflation basin, reaching distances between erosion walls of 54 m, and 159 m between the throat to the end of the deposition lobe. The latter has migrated landward by 39.6 m, i.e., by 7.2 m/yr on average. An average (maximum) vertical erosion within the deflation basin is 2.4 m (5.9 m), with an average (maximum) vertical accretion of 1.95 m (4.7 m) in the deposition lobe.

Figure 7. Aerial photograph (**a**) from the front (taken on July 9, 2021, Ph. Quentin Laporte-Fauret), (**b**) from the back (taken on January 15, 2019, Ph. Bruno Castelle) and (**c**) drone-derived orthophotograph of the parabolic dune at l'Anse du Gurp (from the July 9, 2021 survey).

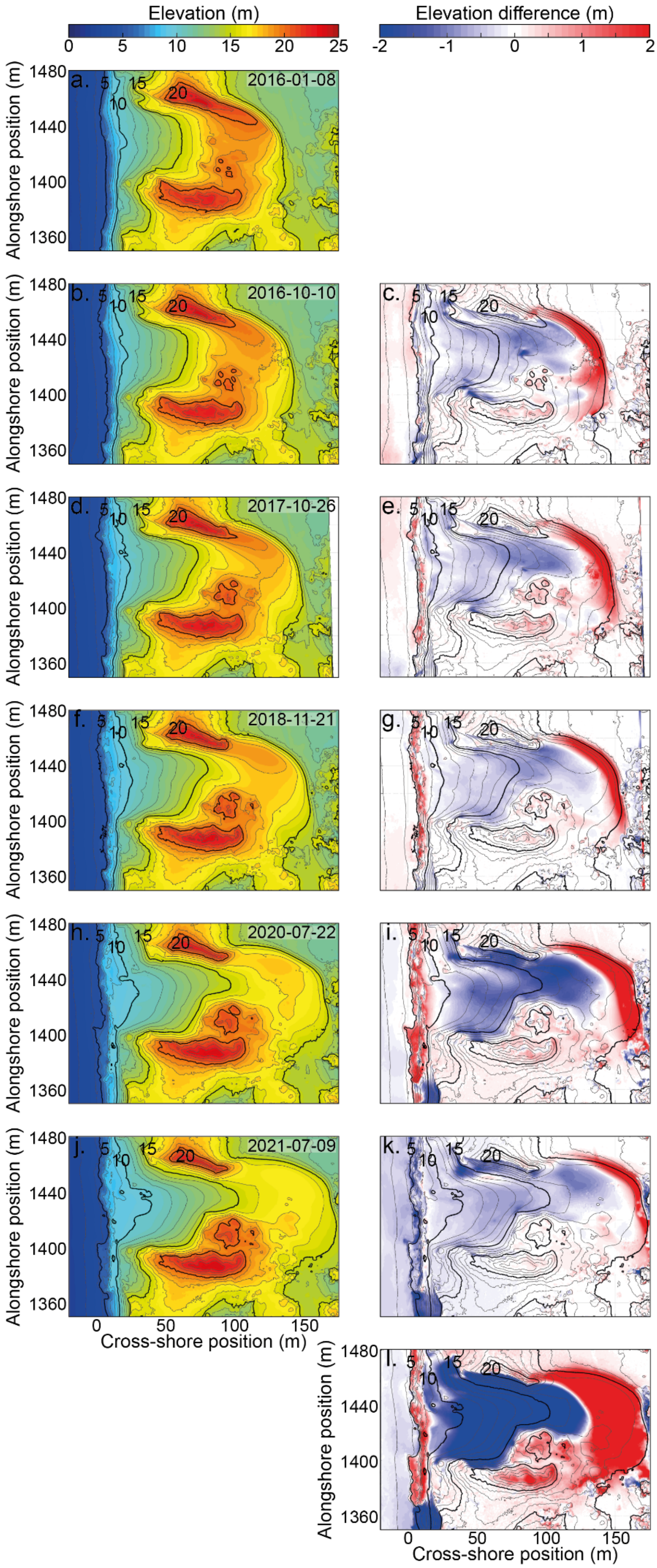

Elevation (m)
0 5 10 15 20 25
Elevation difference (m)
-2 -1 0 1 2
a. 2016-01-08
b. 2016-10-10
c.
d. 2017-10-26
e.
f. 2018-11-21
g.
h. 2020-07-22
i.
j. 2021-07-09
k.
l.
Alongshore position (m)
Cross-shore position (m)

348

Figure 8. (**Left-hand panels**): DSMs of l'Anse du Gurp zoomed onto the parabolic dune from 2016-01-08 to 2021-07-09. (**Right-hand panels**): Elevation difference between two consecutive surveys. (**I**) Net elevation difference between 2016-01-08 and 2021-07-09. All these DSMs were performed by UAV photogrammetry.

Figure 9 shows the 2014-2021 morphological evolution (i.e., cross-shore profile, volume difference and alongshore-averaged shoreline position) of the parabolic dune system (green area in Figure 9.a), compared to two adjacent control areas in the north (blue area in Figure 9.a) and in the south (orange area in Figure 9.a). The cross-shore profiles in the central area (green curves in Figure 9.b) highlight the landward migration (by approximately 40 m) of the deposition lobe with crest lowering (up to 3.3 m). The northern profiles (blue curves in Figure 9.b) are characterized by a dune toe retreat by 4.9 m. The dune crest migrated landward by 3.2 m and raised by 1.14 m. The northern and central profiles are characterized by an approximately 5-m high erosion scarp with a slope break around elevation $z = 9.5$ m. The southern profiles (orange curves in Figure 9.b) show a retreat of the dune toe by 5.5 m, with the dune crest migrating landward by 7 m and lowering by 1.14 m. Contrary to the two other zones, the profile of the southern zone does not show any break in slope around $z = 10$ m, with a steep 17.3-m high face from the shoreline to the crest.

The time series of volume differences show three periods with different evolution patterns (Figure 9.c). During the first period (i.e., from 2014 to the beginning of winter 2017-2018) the northern, the central and the southern areas all show a small decrease in dune volume with seasonal variation amplitude of approximatively 10 m^3/m. At the end of the winter of 2017-2018, the northern, the central and the southern areas all show an increased volume loss by 13.8 m^3/m, 14.5 m^3/m and 21.3 m^3/m, respectively. During the second period (i.e., from the end of the winter of 2017-2018 to July 2020), the dune volume of the southern area has remained relatively stable, while the northern and central areas, although located in slightly more chronically eroding sectors, largely recovered with the dune volume even exceeding that in 2014. The third period (i.e., from July 2020 to July 2021) shows an alongshore quasi-uniform dune volume decrease, with 19.5 m^3/m for the southern area, 23.4 m^3/m for the northern and 27 m^3/m for the central areas. Thus, over the study period, the dune volume decreased by 23.4 m^3/m (i.e., -1.75%), 33 m^3/m (i.e., -2.03%) and 40.1 m^3/m (i.e., -3.72%) for the northern, the central, and the southern areas, respectively.

The three distinct time periods described above are also found in the evolution of the alongshore-averaged shoreline position (Figure 9.d). The first period (i.e., from 2014 to the beginning of winter of 2017-2018) shows relatively stable alongshore-averaged shoreline position for the three areas with some seasonal variations in the order of 1.5 m. The winter of 2017-2018 induced a 1.67 m retreat of the alongshore-averaged shoreline position of the southern area, whereas during the second period (i.e., from the end of the winter 2017-2018 to July 2020) the alongshore-averaged shoreline position of the southern area remained relatively stable. During the same period, the northern and central areas show a seaward shoreline migration by 1.20 m and 4.25 m, respectively. The alongshore-averaged shoreline position of the three areas migrated landward by about 2 m during the third period (i.e., from July 2020 to July 2021). Thus, over the study period, the alongshore-averaged shoreline position eroded by 2.51 m and 5.84 m, for the northern and southern areas respectively, and migrated seaward by 0.65 m for the central area where the parabolic dune is observed, which will be discussed in the next section.

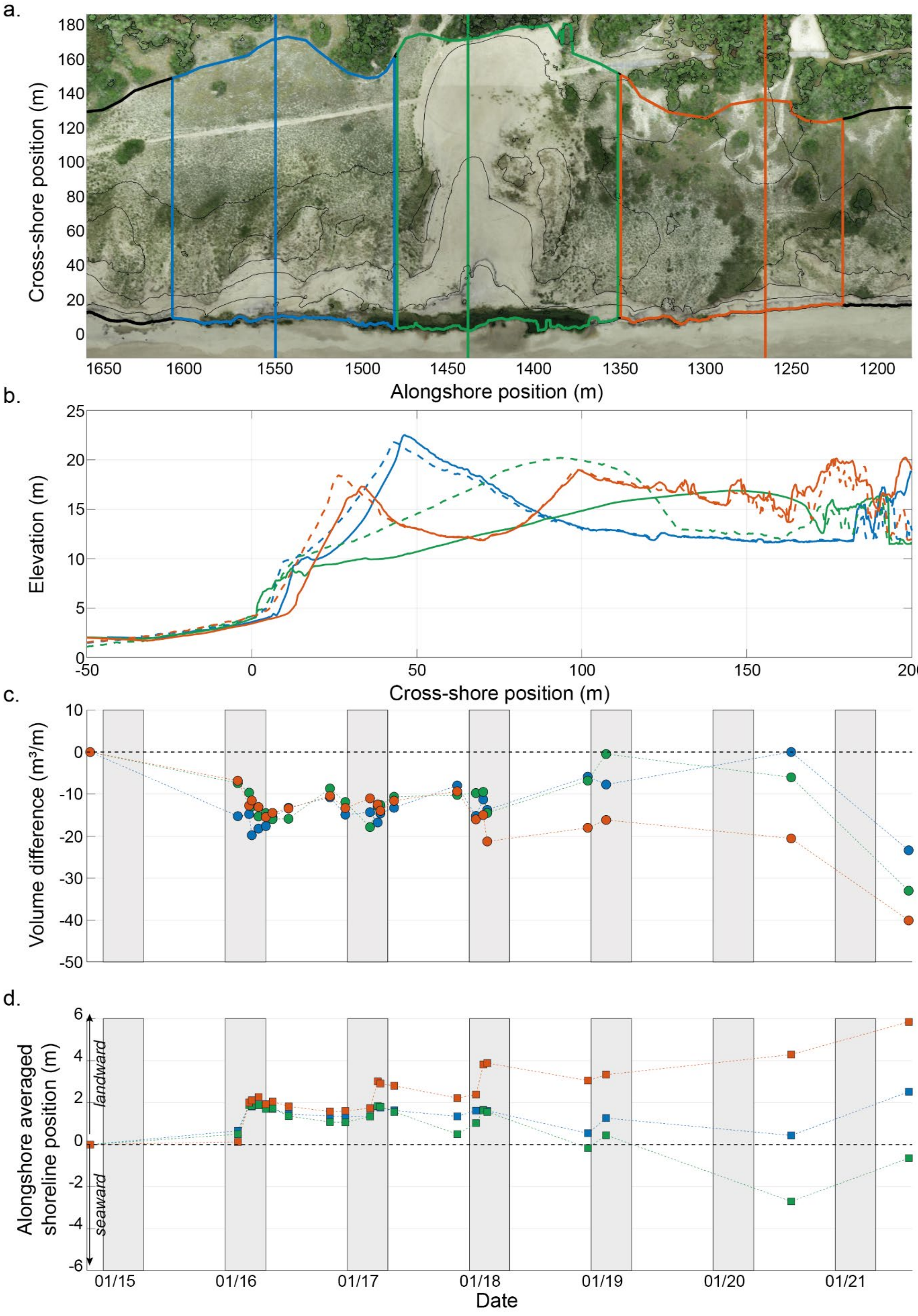

394
395 Figure 9. (**a**) Orthophoto of l'Anse du Gurp zoomed onto the parabolic dune in 2021-07-09. The green
396 area includes the parabolic dune whereas the blue and orange areas are adjacent control areas at the
397 north and south of the parabolic dune, respectively, (**b**) Representative cross-shore profile of each area

(which locations are represented by vertical lines in Figure 9.a), dashed and solid lines are for 2014-10-23 and 2021-07-09, respectively. Time series of (**c**) volume difference and (**d**) alongshore-averaged shoreline position difference in each area. Grey rectangles represent the winter periods.

4. Discussion

The main objective of this study was to investigate the morphological evolution of a freely evolving dune system dissected by blowouts at different stages of development, and the role of blowouts in sediment transfer to the back of the dune, in a chronical erosion context exceeded 2 m/yr since at least 1947.

4.1. Historical blowout evolution

The lifetime of blowouts is dictated by the interactions between physical and biological processes. A blowout can be considered no longer active when enough vegetation is present to overwhelm physical processes (e.g., erosion of the deflation basin) (Schwarz et al., 2018). Jewell et al. (2017) attempted to characterize the initiation and stabilization phases of foredune blowouts in two sites on the Texas coast (USA) between 1969 and 2010. Over 41 years of monitoring, they highlighted at least five phases of foredune recovery (i.e., defined as the expansion of vegetation in the deflation basin) and blowout reactivation, each of them lasting about five years at the first site, and four phases lasting about 10 years at the second site. The blowout reactivation can occur after severe storms, with strong and funneled winds rapidly locally eroding the dune where there is disruption of vegetation. At our study site, the oldest blowout developed in 1977 and was active until 2012 when vegetation began to colonize the deposition lobe and then the deflation basin. Its evolution is currently primarily controlled by biotic processes (i.e., ecological stage in the model of Schwarz et al., 2018). The northern blowout developed between 2004 and 2009 and vegetation began to colonize the southern part of the deposition lobe in 2012 (Figure 4. g-i). It currently appears to be in the bio-morphological stage but if the current physical conditions persist over time, it is possible that this blowout will stabilize because of its limited development space with the presence of the forest to the east, and the chronic marine erosion of the dune to the west. It is also possible that the blowout will disappear due to coastal erosion, which is severe in the north of the study site. Indeed, from 2009 to 2021, the deposition lobe migrated landward by 2.15 m/yr while the shoreline erosion rate reached 3.65 m/yr. Finally, the third blowout that formed between 2004 and 2009 is still active as it developed into a parabolic dune. Its evolution is mainly controlled by physical processes (i.e., geomorphologic stage) preventing the establishment of vegetation. Contrary to Jewell et al. (2017), we therefore did not observe any reactivation phases in any of the three blowouts. It is possible that our time series is too short to capture reactivation phases as blowout lifetime at l'Anse de Gurp could be longer, i.e., decades. Indeed, Girardi and Davis (2010) have highlighted stabilization and reactivation phases over several decades (i.e., three episodes of reactivation between 1969 and 2001) through their GPR monitoring and aerial photography in the northeast coast of the USA. Another explanation is related to the local wave and wind climate. The low-energy conditions of the Texas coast favor stabilization, and occasionally isolated cyclonic events drive reactivation, while the southwest coast of France is a storm-dominated environment. Local climate drives wind, precipitation, waves which in turn influence sand transport (i.e., erosion/deposition) and vegetation dynamics (i.e., growth, colonization) which, in addition to e.g., dune size and shape or chronic marine erosion, are crucial elements to consider in the blowout life cycle (Gonzáles-Villanueva et al., 2011; Hesp, 2002; Schwarz et al, 2018). Finally, as described by Jackson et al. (2019) and Gao et al. (2020), worldwide, and particularly in temperate climates, coastal dunes tend to stabilize due to global increases in temperature, precipitation, and greenhouse gases that result in increased vegetation cover.

4.2. Recent morphological evolution

The volumetric analyses of the dune system between 2014 and 2021 (Figure 6.b) are discussed in the frame of the 2013-2014 winter, which was a winter characterized by extreme storm clustering along the Atlantic coast of Europe driving large-scale coastal erosion (Masselink et al., 2016; Dodet et al., 2019). During the first years of monitoring, the dune volume showed some seasonal variations with a decrease during winters and a recovery the rest of the year. Volume evolution shows some interannual variability, although less pronounced than further south along the coast at Truc Vert (Laporte-Fauret et al., 2020) where the shoreline has been relatively stable over the last decades (Castelle et al., 2018; Robin et al., 2020). However, two winters, 2017-2018 and particularly 2020-2021, appear to have had a larger erosive impact in terms of dune volume (Figure 9.c), which is negatively correlated with shoreline erosion (Figure 9.d). These two winters are both associated with a positive (+1.0 and +0.59 for the winters of 2017-2018 and 2020-2021, respectively) WEPA index (Castelle et al., 2017), which reflects a stormy winter in this region. However, the winter of 2019-2020 was also stormy (WEPA of +0.95), as evidenced in Laporte-Fauret et al. (2021b) by the largest integrated onshore windblown sand flux over at least the last 17 years and the large coastal dune changes observed at Truc Vert. At this stage it is unclear why this 2019-2020 winter had a limited impact on the coastal dune at l'Anse du Gurp, which will need further study.

Interestingly, although chronic shoreline erosion is less intense in the south, the area in the south of the parabolic dune is losing more sediment than the two other areas (Figure 9.b,c). Ignoring the last winter, the central (parabolic dune) and northern areas even show an almost full recovery to their 2014 dune volumes, mostly by either rising in elevation (i.e., northern area) or by migrating landward (i.e., central area – parabolic dune). In these two areas, the shoreline erosion is (more than) compensated by landward transport. On the contrary, the decrease in dune volume and the shoreline landward migration in the southern part seems to characterize an erosion of the dune according to the conceptual model of Sherman and Bauer (1993). An explanation can be that higher erosion scarp in the southern area (i.e., steep 17.3-m high from the shoreline to the crest) limits the transport of windblown sand from the beach to the dune, thus preventing its growth and landward migration (Castelle et al., 2019). Accordingly, erosion scarp height appears to be an important parameter for the landward transport in sectors with roughly similar chronic erosion rate (Davidson et al., 2020). Another factor controlling the dune response is the dense and high vegetation at the dune toe that has grown on the paleosols. These paleosols, which outcropped after the outstanding winter of 2013-2014, are more resistant to marine erosion than sand (Stéphan et al., 2019; Verdin et al., 2019), with fresh groundwater resurgence also favoring dense plant growth (i.e., reeds, Figure 10.c). The dense and high vegetation promotes windblown sand trapping and consolidates the underground by rhizomes system (see review of McGuirk et al., 2022). This rapid growth since approximately 2017 is evidenced by the large accretion patterns facing the parabolic dune (central area) in the DSM difference plot (Figure 8). This vegetation is also present, although less dense, along the northern area (Figure 10.a, b). In contrast, such vegetation is restricted to an isolated patch along the southern, more eroding, area (Figure 10.d). By comparing the nearly concurrent UAV-DSM (July 9, 2021) and Lidar-DEM (October 07, 2021), a correction was applied to the UAV-DSM from October 26, 2017. The estimated vegetation volume facing the parabolic dune (central area) reaches 5.68 m^3/m (Figure 11), which is minor compared to the total volume differences computed in Figure 9.c, and with vegetation volume in the other two areas an order of magnitude smaller (Figure 11). However, it is possible that vegetation height and density impacted the landward dune evolution and volume change by preventing the sand transport from the beach to the deposition lobe. Thus, without new sand input, the deposition lobe may only be fed by the deflation basin with dune volume either constant or slightly decreasing. The latter is especially true during winter storms causing diffuse deposition landward from the deposition lobe). In contrast, the effect of this vegetation on the alongshore-averaged shoreline position time series is more complex to estimate due to the lack of Lidar surveys between 2017 and 2021. Looking only at the differences between the latest drone and lidar surveys, the alongshore-averaged shoreline position difference for the central zone was 1.56 m, highlighting that there is not a seaward shoreline migration of 0.65 m (Figure 9.d), but a landward migration of 0.91 m. As the effect of vegetation is negligible in the northern and southern areas, the slight seaward migration is characteristic of light summer recovery periods related to less marine erosive action. Finally, the alongshore-averaged shoreline position is characterized by a landward migration for the three areas, the central area retreating 2.4 times less and 5.7 times less than the northern and southern areas, respectively. Accordingly, this vegetation, which location and density is strongly controlled by local paleosol characteristics, is critical to local multi-year shoreline erosion.

Our results provide new insight into potential coastal dune management methods in chronically eroding areas. In our study zone, blowouts can help the dune to maintain by migrating landward. Such process is limited if the erosion scarp is high, thus acting as a natural barrier for landward sediment transport from the beach into the dunes. This strategy of coastal dune remobilization is debated because some authors see it as human intervention that alters the landscape and interferes with natural processes, and argue that nature should be left alone (Delgado-Fernandez et al., 2019). On the contrary, other authors defend this remobilization strategy and see it as a way to promote dynamic processes stopped by plant succession and artificial stabilization in order to create a mosaic of vegetated dunes (Creer et al., 2020; Pye and Blott, 2020; Arens et al., 2020). Finally, according to Arens et al. (2020), dune management is not about making good or bad choices. Each choice is valid as long as it is based on a good understanding of the system. Through our study, we believe that in the chronically eroding sectors of southwest France, these blowouts can develop and thus promote landward dune migration, they will evolve through the ecological stage described by Schwarz et al. (2018) and eventually reach stabilization. Such dune migration should allow the dune system to survive on the long term, in contrast with some coastal dunes a couple of kilometers further north in more rapidly eroding sectors, which have now disappeared. However, such blowout systems should be carefully monitored and management action should be taken (e.g., wind fences) to stabilize the parabolic dunes that migrate too far landward. Such controlled dynamism strategy, which could also include lowering the dune scarp by mechanically smoothing the scarp crest, appears as an interesting coastal management avenue in chronically eroding sectors. However, it is necessary to conduct other quantitative studies in different settings worldwide to draw conclusions.

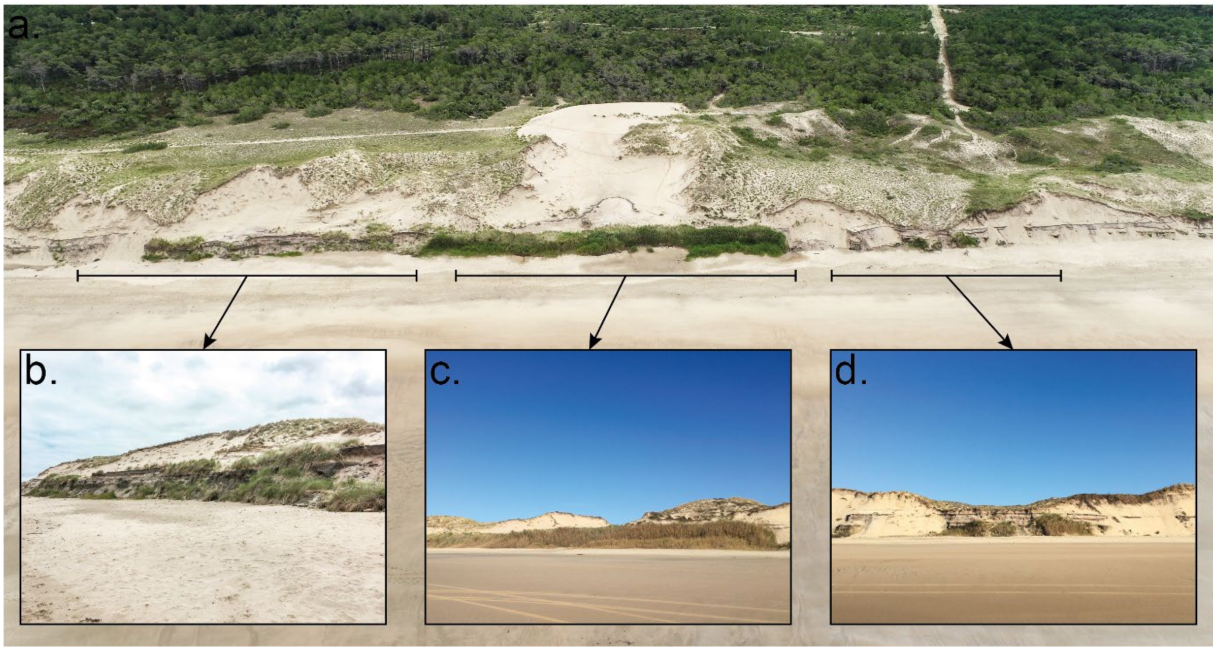

Figure 10. (**a**) Aerial photograph of the parabolic dune and of the adjacent areas in l'Anse du Gurp, photography taken from the beach highlighting the presence (or absence) of vegetation and paleosols near the dune toe at the (**b**) northern, (**c**) central and (**d**) southern zone. Photos **a-b** were taken on July 9, 2021 (Ph. Quentin Laporte-Fauret) and photos **b-c** were taken on November 10, 2021 (Ph. Bruno Castelle).

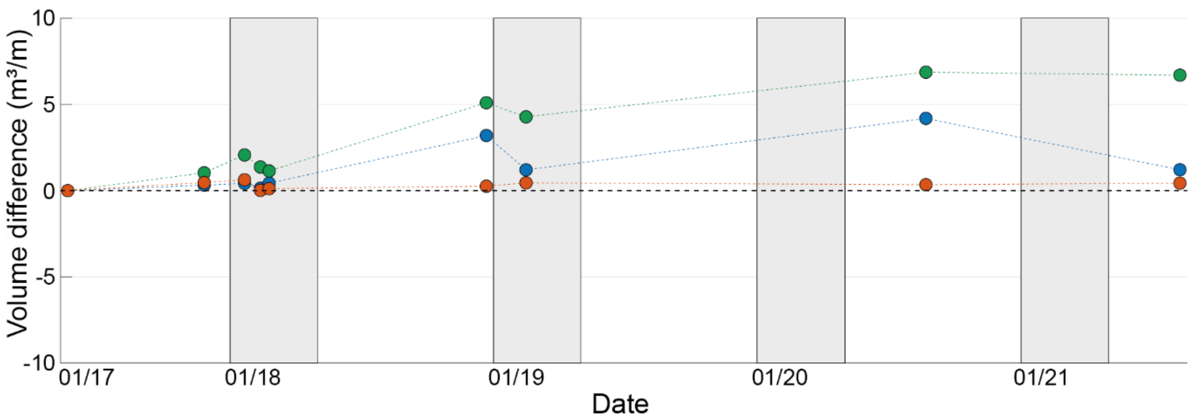

Figure 11. Time series of the volume difference of the vegetation in front of the northern (blue line), central (green line) and southern (orange line) areas from 2017-04-20 to 2021-07-09. Grey rectangles represent the winter periods.

5. Conclusion

The 70-year evolution of a 2-km long high-energy, chronically eroding (average of 1.26 m/yr), coastal dune system has been studied by combining historical aerial photographs, Lidar and UAV surveys. During this period, three major blowouts have developed, all in the northern, more chronically eroding, sector. Two of these blowouts have been stabilized by vegetation colonization or are currently stabilizing, and the third one rapidly evolved into a parabolic dune, which is still migrating into the inland forest. No blowout reactivation phase was observed. Focusing on the 3D evolution of the blowout that recently developed into a parabolic and its adjacent sectors, we found that the blowout promoted dune inland migration. Despite the southern area (no blowout) was in a less chronically eroding sector, the dune volume in this area decreased by the largest amount during the last seven years of high-frequency surveys. This can be explained by the presence of the highest erosion scarp in this area, thus limiting the beach sand transport to the dune. Finally, paleosols outcropping at the dune toe and fresh groundwater resurgence favoring dense plant growth, can also limit marine erosion but also sand transfer from the beach to the dune, which could not be addressed here. Further research in other coastal dune settings is required to explore if and how management of blowout dynamics and potentially scarp lowering/incising can be a relevant coastal dune management strategy in chronically eroding sectors, in order to maintain the coastal dune systems and its ecosystem services.

Author Contributions

Conceptualization, Q.L.-F., V.M. and B.C.; Formal analysis, Q.L.-F.; Funding acquisition, B.C.; Investigation, Q.L.-F., V.M., and B.C.; Methodology, Q.L.-F., V.M. and B.C.; Validation, Q.L.-F.; Writing—original draft, Q.L.-F.; Writing-review & editing, V.M., R.M., B.C., A.N.L. and D.R.

Funding

This research was funded by Agence National de la Recherche (ANR) grant ANR-17-CE01-0014 (SONO project).

Acknowledgments

This research was funded by Agence National de la Recherche (ANR) grant ANR-17-CE01-0014 (SONO project). Additional funding was provided by Observatoire Aquitain des Sciences de l'Univers (OASU) and Observatoire de la Côte de Nouvelle-Aquitaine (OCNA) which also provide LiDAR data. Storage resources for this study was provided by the computing facilities MCIA (Mésocentre de Calcul Intensif Aquitain) of Univ. Bordeaux and Univ. Pau et Pays de l'Adour.

Conflicts of Interest

The authors declare no conflicts of interest.

References

Abhar, K.C., Walker, I.J., Hesp, P., Gares, P.A. (2015). Spatial-temporal evolution of aeolian blowout dunes at Cape Cod Geomorphology, 236, 148-162.

Adamson, D.A., Selkirk, P.M., Colhoun, E.A. (1988). Landforms of aeolian, tectonic and marine origin in the Bauer Bay—Sandy Bar region of subantarctic Macquarie Island. Papers and Proceedings of the Royal Society of Tasmania, 122, 65-82.

Arens, S.M., de Vries, S., Geelen, L.H., Ruessink, G., van der Hagen, H.G., Groenendijk, D. (2020). Comment on 'Is 're-mobilisation' nature restoration or nature destruction? A commentary' by I. Delgado-Fernandez, R.G.D. Davidson-Arnott & P.A. Hesp. J Coast Conserv., 24 (2), 17.

Arens, S.M., Mulder, J.P.M., Slings, Q.L., Geelen, L.H.W.T., Damsma, P. (2013). Dynamic dune management, integrating objectives of nature development and coastal safety: Examples from the Netherlands. Geomorphology, 199, 205–213.

Baas, A.C.W., Nield, J.M. (2007). Modeling vegetated dune landscapes. Geophysical Research Letters, 34(6), L06405.

Barbour, M., Jong, T., Pavlik, B. Marine beach and dune plant communities. In Physiological Ecology of North American Plant Communities; Chabot, B., Mooney, H., Eds.; Chapman & Hall and Methuen: New York, NY, USA, 1985; 296–322.

Black, R.F. (1951). Eolian deposits of Alaska. Arctic, 4, 89–111.

Boak, E.H., Turner, I.L. (2005). Shoreline definition and detection: a review. J. Coast. Res. 21 (4), 688e703.

Bosq M., Bertran P., Beauval C., Kreutzer S., Duval M., Bartz M., Mercier N., Sitzia L., Stéphan P. (2019). Stratigraphy and chronology of Pleistocene coastal deposits in Northern Aquitaine, France: a reinvestigation. Quaternaire, 30, 5-20.

Bossard, V., Lerma, A.N. (2020). Geomorphologic characteristics and evolution of managed dunes on the South West Coast of France, Geomorphology, 367, 107312.

Buffault, P. (1942). Histoire des dunes maritimes de la Gascogne. Editions Delmas, 444p.

Carter, R.W.G., Hesp, P.A., Nordstrom, K.F. (1990). Erosional landforms in coastal dunes. In: Nordstrom, K.F., Psuty, N.P., Carter, R.W.G., (Eds.), Coastal Dunes: Form and Process. Wiley, London, pp. 217– 249.

Castelle, B., Dodet, G., Masselink, G., Scott, T. (2017). A new climate index controlling winter wave activity along the Atlantic coast of Europe: The West Europe Pressure Anomaly. Geophysical Research Letters, 44 (3), 1384-1392.

Castelle, B., Guillot, B., Marieu, V., Chaumillon, E., Hanquiez, V., Bujan, S., Poppeschi, C. (2018). Spatial and temporal patterns of shoreline change of a 280-km long high-energy disrupted sandy coast from 1950 to 2014: SW France. Estuar. Coast. Shelf Sci., 200, 212–223.

Castelle, B., Laporte-Fauret, Q., Marieu, V., Michalet, R., Rosebery, D., Bujan, S., Lubac, B., Bernard, J.-B., Valance, A., Dupont, P., El Moctar, A.O., Narteau, C. (2019). Nature-based solution along high-energy eroding sandy coasts: Preliminary tests on the reinstatement of natural dynamics in reprofiled coastal dunes. Water, 11(12), 2518.

Castelle, B., Marieu, V., Bujan, S., Splinter, K.D., Robinet, A., Sénéchal, N., Ferreira, S. (2015). Impact of the winter 2013–2014 series of severe Western Europe storms on a double barred sandy coast: beach and dune erosion and megacusp embayments. Geomorphology, 238, 135–148.

Cazenave, A., Dieng, H.B., Meyssignac, B., von Schuckmann, K., Decharme, B., Berthier. E. (2014). The rate of sea-level rise. Nat. Clim. Change, 4, 358-361.

Charbonneau, B.R., Dohner, S.M., Wnek, J.P., Barber, D.; Zarnetske, P., Casper, B.B. (2021). Vegetation effects on coastal foredune initiation: Wind tunnel experiments and field validation for three dune-building plants. Geomorphology, 378, 107594.

Charbonneau, B.R., Wnek, J.P., Langley, J.A., Lee, G., Balsamo, R.A. (2016). Above vs. belowground plant biomass along a barrier island: Implications for dune stabilization. J. Environ. Manage., 182, 126–133.

Clemmensen, L.B., Murray, A.S., Bech, J.H., Clausen, A. (2001). Large-scale aeolian sand movement on the west coast of Jutland, Denmark in late Subboreal to early Subatlantic time—a record of climate change or cultural impact? GFF, 123, 193–203.

Cohn, N., Ruggiero, P., de Vries, S., Kaminsky, G.M. (2018). New insights on coastal foredune growth: The relative contributions of marine and aeolian processes. Geophys. Res. Lett., 45, 4965–4973.

Cooper, W.S. (1958). Coastal Sand Dunes of Oregon and Washington. Geological Society of America - Memoir, 72, pp. 169.

Cooper, W.S. (1967). Coastal Sand Dunes of California. Geological Society of America, Memoir, 101, pp. 131.

Creer, J., Litt, E., Ratcliffe, J., Rees, S., Thomas, N., Smith, P. (2020). A comment on some of the conclusions made by Delgado-Fernandez et al. (2019). "Is 're-mobilisation' nature conservation or nature destruction? A commentary". Journal of Coastal Conservation, 24(3), 29.

Davidson, S.G., Hesp, P.A., Silva, G.M.D. (2020). Controls on dune scarping. Progress in Physical Geography, 44 (6), 923-947. doi: 10.1177/0309133320932880

Delgado-Fernandez, I., Davidson-Arnott, R.G.D., Hesp, P.A. (2019). Is 'remobilisation' nature restoration or nature destruction? A commentary. J Coast Conserv., 23, 1093–1103.

Delgado-Fernandez, I., Smyth, T. A. G., Jackson, D. W. T., Smith, A. B., Davidson-Arnott, R. G. D. (2018). Event-scale dynamics of a parabolic dune and its relevance for mesoscale evolution. Journal of Geophysical Research: Earth Surface, 123, 3084–3100.

Dodet, G., Castelle, B., Masselink, G., Scott, T., Davidson, M., Floc'h, F., Jackson, D., Suanez, S. (2019). Beach recovery from extreme storm activity during the 2013–14 winter along the Atlantic coast of Europe. Earth Surface Processes and Landforms, 44 (1), 393-401.Emery, S.M., Rudgers, J.A. (2014). Biotic and abiotic predictors of ecosystem engineering traits of the dune building grass, Ammophila breviligulata. Ecosphere, 5(7), 1–18.

Fraser, G.S., Bennet, S.W., Olyphant, G.A., Bauch, N.J., Ferguson, V., Gellasch, C.A., Millard, C.L., Mueller, B., O'Malley, P.J., Way, N., Woodfield, M.C. (1998). Wind flow circulation patterns in a coastal dune blowout, south coast of Lake Michigan. Journal of Coastal Research, 14, 451– 460.

Gao, J., Kennedy, D.M., Konlechner, T.M. (2020). Coastal dune mobility over the past century: A global review. Progress in Physical Geography: Earth and Environment, 44 (6), 814-836.

Gares, P.A., Nordstrom, K.F. (1995). A cyclic model of foredune blowout evolution for a leeward coast, Island Beach, New Jersey Ann. Assoc. Am. Geogr., 85 (1), 1-20.

Girardi, J.D., Davis, D.M. (2010). Parabolic dune reactivation and migration at Napeague, NY, USA: insights from aerial and GPR imagery. Geomorphology, 114 (4), 530-541.

Glenn, M. (1979). Glossary. In: McKee, E.D., (Ed.), A Study of Global Sand Seas. United States Geological Survey Professional Paper, 1052. US Gov. Printing Office, Washington, pp. 399– 407.

González-Villanueva, R., Costas, S., Duarte, H., Perez-Arlucea, M., & Alejo, I. (2011). Blowout evolution in a coastal dune: using GPR, aerial imagery and core records. Journal of Coastal Research, (64), 278–282.

Hesp, P. (2002). Foredunes and blowouts: Initiation, geomorphology and dynamics. Geomorphology, 48, 245–268.

Hesp, P., Hilton, M.J. (2013). Restoration of foredunes and transgressive dunefields: case studies from New Zealand. In Restoration of Coastal Dunes; Springer: Berlin, Germany, 2013; pp. 67–92.

Hesp, P., Hyde, R. (1996). Flow dynamics and geomorphology of a trough blowout Sedimentology, 43 (3), 505-525.

Hesp, P., Walker, I.J. (2012). Three-dimensional aeolian dynamics within a bowl blowout during offshore winds, Greenwich Dunes, Prince Edwards Island, Canada. Aeolian Res., 3, 389-399.

Hesp, P. (2001). The Manawatu dune field: environmental change and human impacts. N.Z. Geogr., 57 (2), 33-40.

Hugenholtz, C.H., Wolfe, S.A. (2006). Morphodynamics and climate controls of two aeolian blowouts on the northern Great Plains, Canada Earth Surf. Process. Landf., 31 (12), 1540-1557.

Hugenholtz, C.H., Wolfe, S.A. (2009). Form-flow interactions of an aeolian saucer blowout Earth Surf. Process. Landf., 34 (7), 919-928.

Jackson, D.W.T., Beyers, J.H.M., Cooper, J.A.G., Baas, A.C.W., Delgado-Fernandez, I. (2011). Investigation of three-dimensional wind flow behaviour over a coastal dune morphology under offshore winds using computational fluid dynamics (CFD) and ultrasonic anemometry Earth Surface Processes and Landforms, 36, 1113-1124.

Jackson, D.W.T., Costas, S., González-Villanueva, R., Cooper, A. (2019). A global 'greening' of coastal dunes: An integrated consequence of climate change? Global and Planetary Change, 182, 103026.

Jalón-Rojas, I., Castelle, B. (2021). Climate Control of Multidecadal Variability in River Discharge and Precipitation in Western Europe, Water, 13, 257, doi:10.3390/w13030257.

Jewell, M., Houser, C., Trimble, S. (2017). Phases of blowout initiation and stabilization on Padre Island revealed through ground-penetrating radar and remotely sensed imagery. Phys. Geogr., 1–22.

Jungerius, P.D., van der Meulen, F. (1989). The development of dune blowouts, as measured with erosion pins and sequential air photos Catena, 16, 369-376.

Kuipers, M. (2014). The daring Dutch: restoring the dynamic dunes. In: Favennac, J., Battiau-Queney, Y. (Eds.). Coastal dunes management strategies and practices: perspectives and case studies, vol. 33, Dynamiques environnementales, pp.132–138.

Laporte-Fauret, Q., Alonso Ayuso, A.T., Rodolfo-Damiano, T., Marieu, V., Castelle, B., Bujan, S., Rosebery, D., Michalet, R. (2021a). The role of physical disturbance for litter decomposition and nutrient cycling in coastal sand dunes. Ecological Engineering, 161, 106181.

Laporte-Fauret, Q., Castelle, B., Marieu, V., Michalet, R., Bujan, S., Rosebery. D. (2021b). Morphological and ecological responses of a managed coastal sand dune to experimental notches. Science of the Total Environment, 782, 146813.

Laporte-Fauret, Q., Marieu, V., Castelle, B., Michalet, R., Bujan, S., Rosebery, D. (2019). Low-Cost UAV for High-Resolution and Large-Scale Coastal Dune Change Monitoring Using Photogrammetry. Journal of Marine Science and Engineering, 7(3), 63.

Laporte-Fauret, Q., Castelle, B., Marieu, V., Bujan, S., Michalet, R., Rosebery, D. Coastal dune morphology evolution combining Lidar and UAV surveys, Truc Vert beach 2011–2019. In Global Coastal Issues of 2020. Journal of Coastal Research; Special Issue No. 95; Malvárez, G., Navas, F., Eds.; Coastal Education and Research Foundation, Inc.: Coconut Creek, FL, USA, 2020; pp. 163-167.

Lerma, A.N., Ayache, B., Ulvoas, B., Paris, B., Bernon, N., Bulteau, T., Mallet, C. (2019). Pluriannual beach-dune evolutions at regional scale: Erosion and recovery sequences analysis along the aquitaine coast based on airborne LiDAR data. Continental Shelf Research, 189, 103974.

Livingstone, I., Warren, A. (1996). Aeolian Geomorphology: An Introduction Longman, Harlow

Luijendijk, A., Hagenaars, G., Ranasinghe, R., Baart, F., Donchyts, G., Aarninkhof, S. (2018). The State of the World's Beaches. Sci. Rep., 8, 6641.

Martinez, M.L., Hesp, P., Gallego-Fernandez, J.B. Coastal dunes: Human impact and need for restoration. In Restoration of Coastal Dunes; Martinez, M.L., Gallego-Fernández, J.B., Hesp, P., Eds.; Springer: Berlin/Heidelberg, Germany, 2013, 1–14.

Masselink, G., Castelle, B., Scott, T., Dodet, G., Suanez, S., Jackson, D., Floc'h, F. (2016). Extreme wave activity during 2013/2014 winter and morphological impacts along the Atlantic coast of Europe. Geophys. Res. Lett. 43 (5), 2135–2143.

Maun, M.A. (1998). Adaptations of plants to burial in coastal sand dunes. Can. J. Bot., 76, 713–738.

Maun, M.A., Perumal, J. (1999). Zonation of vegetation on lacustrine coastal dunes: Effects of burial by sand. Ecol. Lett., 2, 14–18.

McGuirk, M.T., Kennedy, D.M., Konlechner, T. (2022). The role of vegetation in incipient dune and foredune development and morphology: A review. Journal of Coastal Research, 38(2), 414–428. Coconut Creek (Florida), ISSN0749-0208.

Melton, F.A. (1940). A tentative classification of sand dunes: its application to dune history in the southern High Plains. Journal of Geology, 48, 113-174.

Merkens, J.L., Lincke, D., Hinkel, J., Brown, S., Vafeidis, A.T. (2018). Regionalization of population growth projections in coastal exposure analysis. Climatic Change, 151 (3-4), 413-426.

Neumann, B., Vafeidis, A.T., Zimmermann, J., Nicholls, R.J. (2015). Future coastal population growth and exposure to sea-level rise and coastal flooding - A global assessment. PLoS ONE, 10 (3), e0131375.

Nield, J.M., Baas, A.C.W. (2008). Investigating parabolic and nebkha dune formation using a cellular automaton modelling approach. Earth Surface Processes and Landforms, 33(5), 724-740.

Nordstrom, K.F. Beaches and Dunes of Developed Coasts; Cambridge University Press: Cambrige, UK, 2000, pp. 347.

Nordstrom, K.F., Hartman, J., Freestone, A.L., Wong, M., Jackson, N.L. (2007). Changes in topography and vegetation near gaps in a protective foredune. Ocean Coast. Manag., 50, 945–959.

Pease, P., Gares, P.A. (2013). The influence of topography and approach angles on local deflections of airflow within a coastal blowout. Earth Surf. Process. Landforms, 38, 1160–1169.

Petersen, J., Janssen, G., Lammers, E.J., Menn, I., Mulder, S. (2005). Beaches and Dunes. In Wadden Sea Quality Status Report 2004; Essink, K., Ed.; CommonWadden Sea Secretariat: Wilhelmshaven, Germany, 2005; pp. 237–258.

Pontee N.I., Tastet J.-P., Massé L. (1998). Morphosedimentary evidence of Holocene coastal changes near the mouth of the Gironde and on the Medoc Peninsula, SW France. Oceanologica Acta, 21 (2), 243-261.

Provoost, S., Jones, M.L.M., Edmondson, S.E. (2011). Changes in landscape and vegetation of coastal dunes in northwest Europe: A review. J. Coast. Conserv., 15, 207–226.

Pye, K., Blott, S.J., Howe, M.A. (2014). Coastal dune stabilization in Wales and requirements for rejuvenation. J. Coast. Conserv., 18, 27–54.

Pye, K., Blott, S.J. (2016). Dune Rejuvenation Trials: Overview Report; Report to Natural Resources Wales. Tech. Rep. KPAL Report 19099; Kenneth Pye Associates Ltd.: Reading, UK.

Pye, K., Blott, S.J. (2017). Evolution of a sediment-starved, over-stabilized dune field: Kenfig Burrows, South Wales, UK. J. Coast. Conserv., 21, 685–717.

Pye, K., Blott, S.J. (2020). Is 're-mobilisation' nature restoration or nature destruction? A commentary. Discussion., Journal of Coastal Conservation, 24(1), 10.

Rhind, P., Jones, R. (2009). A framework for the management of sand dune systems in Wales. J. Coast. Conserv., 13, 15–23.

Robin, N., Billy, J., Castelle, B., Hesp, P., Lerma, A.N., Laporte-Fauret, Q., Marieu, V., Rosebery, D., Bujan, S., Destribats, B., Michalet, R. (2020). 150 years of Foredune initiation and evolution driven by human and natural processes. Geomorphology, 374, 107516.

Ruessink, B., Arens, S., Kuipers, M., Donker, J. (2018). Coastal dune dynamics in response to excavated foredune notches. Aeolian Res., 31, 3–17.

Schwarz, C., Brinkkemper, J., Ruessink, G. (2018). Feedbacks between Biotic and Abiotic Processes Governing the Development of Foredune Blowouts: A Review. J. Mar. Sci. Eng., 7 (1), 2. doi:10.3390/jmse7010002.

Sherman, D.J., Bauer, O. (1993). Dynamics of beach-dune systems. Progress in Physical Geography, 17(4), 413–447.

Smyth, T.A.G., Jackson, D.W.T., Cooper, J.A.G. (2012). High resolution measured and modeled three-dimensional airflow over a coastal bowl blowout Geomorphology, 177-178, 62-73.

Stéphan, P., Verdin, F., Arnaud-Fassetta, G., Bertrand, F., Eynaud, F., García-Artola, A., Bosq, M., Culioli, C., Suanez, S., Coutelier, C., Bertran, P., Costa, S. (2019). Holocene coastal changes along the Gironde estuary (SW France): New insights from the North Médoc peninsula beach/dune system. Quaternaire, 30 (1), 47-75.

Van Boxel, J.H., Jungerius, P.D., Kieffer, N., Hampele, N. (1997). Ecological effects of reactivation of artificially stabilized blowouts in coastal dunes. J. Coast. Conserv., 3, 57–62.

Verdin F., Eynaud F., Stéphan P., Arnaud-Fassetta G., Bosq M., Bertrand F., Suanez S., Coutelier C., Comte F., Wagner S., Belingard C., Ard V., Manen C., Saint-Sever G., Marchand G. (2019). Humans and their environment on the Médoc coastline from the Mesolithic to the roman period. Quaternaire, 30 (1), 77-95.

Wiedemann, A. M. (1991). 'The coastal parabola dune system at Sandlake, Tillamook County, Oregon', in Davidson-Arnott, R. (Ed.), Proc. Symposium on Coastal Sand Dunes, National Research Council Canada, Ottawa, 171-194.

Yan, N., Baas, A. C. (2015). Parabolic dunes and their transformations under environmental and climatic changes: Towards a conceptual framework for understanding and prediction. Global and Planetary Change, 124, 123–148.

Zappa, G., Shaffrey, L.C., Hodges, K.I., Sansom, P.G., Stephenson D.B. (2013). A multi model assessment of future projections of North Atlantic and european extratropical cyclones in the CMIP5 climate models. J. Clim., 26, 5846-5862.

Zarnetske, P.L., Hacker, S.D., Seabloom, E.W., Ruggiero, P., Killian, J.R., Maddux, T.B., Cox, D. (2012). Biophysical feedback mediates effects of invasive grasses on coastal dune shape. Ecology, 93, 1439–1450.